Turkish Online Journal of Qualitative Inquiry (TOJQI)
Volume 12, Issue 9, August 2021: 2932-2947

A Study of Drugs Administered for Medication of COVID-19 and Mucormycosis using KCD Polynomials and Indices

Keerthi G. Mirajkar[a], Akshata Morajkar[b]

[a]Assistant Professor, Department of Mathematics, Karnatak University's Karnatak Arts College, Dharwad.
[b]Research scholar, Department of Mathematics, Karnatak University, Dharwad.

Abstract

The current study computes KCD (Karnatak College Dharwad) indices for the drugs used to treat COVID-19 using KCD polynomials through edge partition technique for considered molecular structures of ivermectin, remdesivir and amphotericin B. Additionally, attention is focused on QSPR/QSAR (quantitative structure property/activity relationship) analysis of these and other drugs to investigate the correlation of their physicochemical properties using degree based topological indices. The conducted study reveals that the considered topological indices show strong positive correlation with the physicochemical properties of analysed drugs used to treat COVID-19 and mucormycosis. The appealing result is the performance of Randić index for mild disease category and black fungus disease, along with first KCD index for moderate/severe disease category showing highest average correlation values for physicochemical properties of these drugs.

Keywords: COVID-19, KCD polynomials, mucormycosis (black fungus), QSPR/QSAR, topological indices.

1. Introduction

The COVID-19 expandable as coronavirus disease 2019 emerged around December 2019 in Wuhan, China (**Lu *et al.*, 2020**). COVID-19 is the consequence of SARS-CoV-2 from betacoronavirus family. Thus world has encountered a huge pandemic since then. The first COVID-19 case in India (outbreak in China) was identified in January 2020 in Kerala (**Ghosh *et al.*, 2020**). The rise in cases was around June-August, with a drop observed from September onwards and a fall towards January 2021 (**Ghosh *et al.*, 2020; Samui *et al.*, 2020**). From mid March 2021 onwards India has experienced the begin of second wave with higher intensity compared to the first wave. By the end of April 2021 India has reached the peak with number of active cases rising per day (**Ranjan *et al.*, 2021**), while a dip in these cases was observed with the end of June 2021. The cause of concern during second wave is the rise in mucormycosis (black fungus) cases due to reducing immunity of COVID-19 patients (**Sahoo *et al.*, 2021**). From the beginning of first wave of COVID-19 and the occurrence of second wave till date India has developed its medical facility in all aspects.

The process of discovering a drug initially involves the identification, followed by rigorous trial and error programs to predict the molecular compound of interest. This involves a large scale of

clincial trials. These processes require a huge investments. To accelerate a drug discovery and reduce the cost of investment these days computer aided drug design (CADD) is highly preferred. In particular, CADD uses the technique of quantitative structure property/activity relationship (QSPR/QSAR) to study the contribution of chemical structure in the physicochemical properties of the compounds. Mathematically, this is attained through correlation between chemical structures and their properties. A QSPR model is developed statistically to understand the dependency between structural characteristics of a compound and their properties. The ability of a QSPR model relies on the structure of a molecule, types of descriptors used and methods used to develop the model.

Descriptors are the representers of a molecule in numerical form. One such descriptor is topological index in the form of graph invariant which encodes the molecular graph's topology. QSPR analysis using topological indices is gaining wide acceptance these days. Recently Hosamani has studied QSPR model of phytochemicals screened against SARS-CoV-2 $3CL^{pro}$ (**Hosamani, 2020**). Later Kirmani *et al*. has analysed COVID-19 drugs using QSPR employing topological indices (**Kirmani *et al*., 2020**).

To avail the use of topological indices the chemical structures are first converted into molecular graphs observing atoms as vertices and bonds connecting atoms as edges (**Balban, 1976**). The graphs considered throughout the study are simple and connected having $|V(G)| = n$ as vertex set and $|E(G)| = m$ as edge set. The edge $e = uv \in G$ connects vertices u and v, let $E(G) = \bigcup_{i=1}^{n} E_i(G)$. $d_G(u)$ represents degree of vertex $u \in G$ and $d_G(e)$ serves as edge degree given by $d_G(u) + d_G(v) - 2$. For undefined terminologies refer (**Harary, 1969**).

The first topological index was developed by Wiener to study the boiling points of alkanes and it was Wiener index (**Wiener, 1947**). The oldest degree based topological index is Randić index (**Randić, 1975**). Gutman *et al*. defined the renowned Zagreb indices (**Gutman *et al*., 1975; Gutman *et al*., 1972**).

2. Motivation

The applications of various topological indices and corresponding polynomials (**Kirmani *et al*., 2020; Hosamani, 2020**) has motivated us to introduce polynomials for KCD indices (**Mirajkar & Morajkar, 2020**) . Thus in the present article we introduce two fresh polynomials in the form of KCD polynomials. Due to the immense medical use of antiviral drugs ivermectin, remdesivir, amphotericin B and others in the treatment of COVID-19, current research investigates the degree based topological indices and KCD polynomials of these molecular structures. Additionally, these antiviral drugs are tested for predictive strength using linear regression model and their correlation with respective to physicochemical properties using Randić index (**Randić,1975**), general Randić index $\left(k = \frac{1}{2}\right)$ (**Bollobás & Erdös, 1998**), geometric-arithmetic index (**Vukičević & Furtula, 2009**) and KCD indices (**Mirajkar & Morajkar, 2020**). The outcomes of present research will serve to understand the physicochemical properties of COVID-19 drugs in a better form.

3. Topological Indices

The first degree based topological index was defined by Randić called Randić index $\boldsymbol{R(G)}$ (**Randić, 1975**), given by

$$R(G) = \sum_{uv \in E(G)} \frac{1}{\sqrt{d_G(u) d_G(v)}} \tag{3.1}$$

Later Bollobas *et al*. defined general Randić index $R_k(G)(k = \frac{1}{2})$ (**Bollobás & Erdös, 1998**) as

$$R_k(G) = \sum_{uv \in E(G)} \sqrt{d_G(u) d_G(v)} \tag{3.2}$$

Vukičević *et al*. defined geometric-arithmetic index $GA(G)$ using geometric mean and arithmetic mean (**Vukičević & Furtula, 2009**) as

$$GA(G) = \sum_{uv \in E(G)} \frac{2\sqrt{d_G(u) d_G(v)}}{d_G(u) + d_G(v)} \tag{3.3}$$

Mirajkar *et al*. defined First KCD index $KCD_1(G)$ and second KCD index $KCD_2(G)$ (**Mirajkar & Morajkar, 2020**) as

$$KCD_1(G) = \sum_{e=uv \in E(G)} ((d_G(u) + d_G(v)) + d_G(e)) \tag{3.4}$$

$$KCD_2(G) = \sum_{e=uv \in E(G)} (d_G(u) + d_G(v)) d_G(e). \tag{3.5}$$

4. Methodology

The list of antiviral drugs suggested by AIIMS (All India Institute of Medical Sciences)/ICMR-COVID-19 (Indian Council of Medical Research) National Task Force/Ministry of Health and Family Welfare, Government of India dated $22nd$ April 2021 and Government of Karnataka dated $01st$ May 2021 for the medication of adult COVID-19 patients along with drugs adviced by IMA (Indian Medical Association) for treating mucormycosis are used for the current research study. The molecular structures of these drugs and their physicochemical properties mentioned in tables 4, 7 and 10 are assembled from https://pubchem.ncbi.nlm.nih.gov. The molecular graphs of these molecular structures are hydrogen suppressed. To attain the results degree counting method, edge partition method and analytical techniques are utilized. Initially the edge partitions of molecular graphs is carried out using the degree of end vertices. Later, the results are computed using edge partitions. R-software is applied to obtain the linear regression model for QSPR analysis and graphs are plotted using Ms-Excel.

5. KCD Polynomials

Graph polynomials are used to measure the structural information of graphs. The idea behind its use is to compute the required information in more efficient manner. Several graph polynomials have been studied in graph theory. Hosoya initiated the use of polynomials to obtain topological indices by defining Hosoya polynomial in 1988, whose first derivative at $x = 1$ gives Wiener index (**Hosoya, 1971**). The computation of Hosoya polynomial for some molecular graphs are available in (**Gutman *et al*., 2001; Stevanović, 2001**). Later, Fath-Tabar established first and second Zagreb

polynomials (**Fath-Tabar, 2009**). These graph polynomials prove to be a powerful tool to encode the knowledge of the graphs.

In this segment we define the KCD polynomials for KCD indices given by Eqs. (3.4) and (3.5). Also computation of KCD polynomials for the drugs used in the treatment of COVID-19 and black fungus disease: ivermectin, remdesivir and amphotericin B compounds are covered.

The first KCD polynomial $KCD_1(G,x)$ of G is

$$KCD_1(G,x) = \sum_{e=uv\in E(G)} (x^{d_G(u)+d_G(v)} + x^{d_G(e)}) \tag{5.1}$$

The second KCD polynomial $KCD_2(G,x)$ of G is

$$KCD_2(G,x) = \sum_{e=uv\in E(G)} (d_G(u) + d_G(v))x^{d_G(e)} \tag{5.2}$$

It is observable that the first derivative of Eqs. (5.1) and (5.2) at $x = 1$ generates $KCD_1(G)$ and $KCD_2(G)$ respectively.

5.1 KCD Polynomials of Ivermectin

Graph I in figure 1 represents the molecular graph of ivermectin. It has $|V(I)| = 62$ and $|E(I)| = 67$. For $i,j \geq 1$, $uv \in E(I)$ and $(d_I(u), d_I(v)) = (i,j)$ and let $E(I) = \bigcup_{i=1}^{8} E_i(I)$.

Figure.1 Molecular graph of ivermectin.

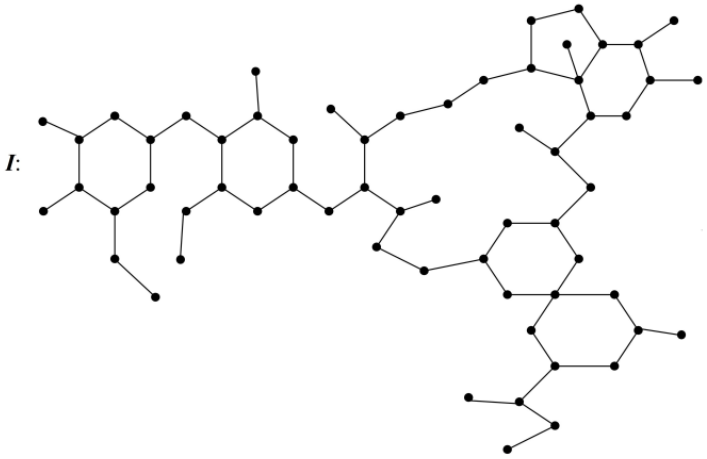

Table.1 Edge partition of $E(I)$.

$E_i = E_i(I)$	$d_I(u) = i$	$d_I(v) = j$	$d_I(e)$	$\lvert E_i(I)\rvert$
E_1	1	2	1	3
E_2	1	3	2	9
E_3	1	4	3	1
E_4	2	2	2	5
E_5	2	3	3	31
E_6	2	4	4	4
E_7	3	3	4	11
E_8	3	4	5	3

Theorem 5.1 *For the molecular graph of ivermectin,*

$a.)\ KCD_1(I,x) = 3x^7 + 15x^6 + 35x^5 + 29x^4 + 35x^3 + 14x^2 + 3x \ and\ \ KCD_1(I) = 538.$

$b.)\quad KCD_2(I,x) = 21x^5 + 90x^4 + 160x^3 + 56x^2 + 9x \quad and \quad KCD_2(I) = 1066.$

Proof. With the help of Eq. (5.1) and table 1, we obtain

$$KCD_1(I,x) = \sum_{e=uv\in E(I)} (x^{d_I(u)+d_I(v)} + x^{d_I(e)})$$

$$= (\sum_{e=uv\in E_1(I)} + \sum_{e=uv\in E_2(I)} + \sum_{e=uv\in E_3(I)} + \sum_{e=uv\in E_4(I)} + \sum_{e=uv\in E_5(I)} + \sum_{e=uv\in E_6(I)} + \sum_{e=uv\in E_7(I)} + \sum_{e=uv\in E_8(I)})\big((d_I(u) + d_I(v))x^{d_I(e)}\big)$$

$$= (|E_1(I)| + |E_2(I)| + |E_3(I)| + |E_4(I)| + |E_5(I)| + |E_6(I)| + |E_7(I)| + |E_8(I)|)\big(x^{d_I(u)+d_I(v)} + x^{d_I(e)}\big)$$

$$= 3(x^3 + x) + 9(x^4 + x^2) + (x^5 + x^3) + 5(x^4 + x^2) + 31(x^5 + x^3) + 4(x^6 + x^4) + 11(x^6 + x^4) + 3(x^7 + x^5)$$

$$= 3x^7 + 15x^6 + 35x^5 + 29x^4 + 35x^3 + 14x^2 + 3x.$$

$KCD_1(I)$ being first derivative of $KCD_1(I,x)$ at $x = 1$, gives

$$KCD_1(I) = \frac{\partial}{\partial x}(KCD_1(I,x))|_{x=1}$$

$$= \frac{\partial}{\partial x}(3x^7 + 15x^6 + 35x^5 + 29x^4 + 35x^3 + 14x^2 + 3x)|_{x=1}$$

$$= 538.$$

Using Eq. (5.2) and table 1, we get

$$KCD_2(I,x) = \sum_{e=uv\in E(I)} (d_I(u) + d_I(v))x^{d_I(e)}$$

$$= (\sum_{e=uv\in E_1(I)} + \sum_{e=uv\in E_2(I)} + \sum_{e=uv\in E_3(I)} + \sum_{e=uv\in E_4(I)} + \sum_{e=uv\in E_5(I)} + \sum_{e=uv\in E_6(I)} + \sum_{e=uv\in E_7(I)} + \sum_{e=uv\in E_8(I)})\big((d_I(u) + d_I(v))x^{d_I(e)}\big)$$

$$= (|E_1(I)| + |E_2(I)| + |E_3(I)| + |E_4(I)| + |E_5(I)| + |E_6(I)| + |E_7(I)| + |E_8(I)|)\big((d_I(u) + d_I(v))x^{d_I(e)}\big)$$

$$= 3(3x) + 9(4x^2) + (5x^3) + 5(4x^2) + 31(5x^3) + 4(6x^4) + 11(6x^4) + 3(7x^5)$$

$$= 21x^5 + 90x^4 + 160x^3 + 56x^2 + 9x.$$

$KCD_2(I)$ being first derivative of $KCD_2(I,x)$ at $x=1$, gives

$$KCD_2(I) = \frac{\partial}{\partial x}(KCD_2(I,x))|_{x=1}$$
$$= \frac{\partial}{\partial x}(21x^5 + 90x^4 + 160x^3 + 56x^2 + 9x)|_{x=1}$$
$$= 1066.$$

5.2 KCD Polynomials of Remdesivir

Graph R in figure 2 represents the molecular graph of remdesivir. It has $|V(R)| = 41$ and $|E(R)| = 44$. For $i,j \geq 1$, $uv \in E(R)$ and $(d_R(u), d_R(v)) = (i,j)$ and let $E(R) = \cup_{i=1}^{8} E_i(R)$.

Figure.2 Molecular graph of remdesivir.

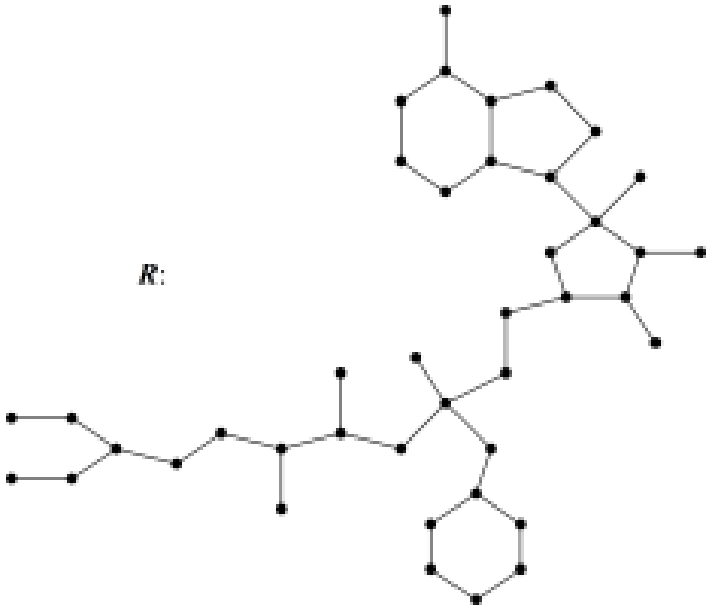

Table. 2 Edge partition of $E(R)$.

$E_i = E_i(R)$	$d_R(u) = i$	$d_R(v) = j$	$d_R(e)$	$\lvert E_i(R)\rvert$
E_1	1	2	1	2
E_2	1	3	2	5
E_3	1	4	3	2
E_4	2	2	2	9
E_5	2	3	3	14
E_6	2	4	4	4
E_7	3	3	4	6
E_8	3	4	5	2

Theorem 5.2 *For the molecular graph of remdesivir,*

$a.)\quad KCD_1(R,x) = 2x^7 + 10x^6 + 18x^5 + 24x^4 + 18x^3 + 14x^2 + 2x \; and$

$KCD_1(R) = 344.$

$b.)\quad KCD_2(R,x) = 14x^5 + 60x^4 + 80x^3 + 56x^2 + 6x \quad and \quad KCD_2(R) = 668.$

Proof. With the help of Eq. (5.1) and table 2, we obtain

$$KCD_1(R,x) = \sum_{e=uv\in E(R)} (x^{d_R(u)+d_R(v)} + x^{d_R(e)})$$

$$= (\sum_{e=uv\in E_1(R)} + \sum_{e=uv\in E_2(R)} + \sum_{e=uv\in E_3(R)} + \sum_{e=uv\in E_4(R)} + \sum_{e=uv\in E_5(R)} + \sum_{e=uv\in E_6(R)} + \sum_{e=uv\in E_7(R)} + \sum_{e=uv\in E_8(R)})\left(x^{d_R(u)+d_R(v)} + x^{d_R(e)}\right)$$

$$= (|E_1(R)| + |E_2(R)| + |E_3(R)| + |E_4(R)| + |E_5(R)| + |E_6(R)| + |E_7(R)| + |E_8(R)|)\left(x^{d_R(u)+d_R(v)} + x^{d_R(e)}\right)$$

$$= 2(x^3 + x) + 5(x^4 + x^2) + 2(x^5 + x^3) + 9(x^4 + x^2) + 14(x^5 + x^3)$$

$$+4(x^6 + x^4) + 6(x^6 + x^4) + 2(x^7 + x^5)$$

$$= 2x^7 + 10x^6 + 18x^5 + 24x^4 + 18x^3 + 14x^2 + 2x.$$

$KCD_1(R)$ being first derivative of $KCD_1(R,x)$ at $x = 1$, gives

$$KCD_1(R) = \frac{\partial}{\partial x}(KCD_1(R,x))|_{x=1}$$

$$= \frac{\partial}{\partial x}(2x^7 + 10x^6 + 18x^5 + 24x^4 + 18x^3 + 14x^2 + 2x)|_{x=1}$$

$$= 344.$$

Using Eq. (5.2) and table 2, we get

$$KCD_2(R,x) = \sum_{e=uv\in E(R)} (d_R(u) + d_R(v))x^{d_R(e)}$$

$$= (\sum_{e=uv\in E_1(R)} + \sum_{e=uv\in E_2(R)} + \sum_{e=uv\in E_3(R)} + \sum_{e=uv\in E_4(R)} + \sum_{e=uv\in E_5(R)} + \sum_{e=uv\in E_6(R)} + \sum_{e=uv\in E_7(R)} + \sum_{e=uv\in E_8(R)})\left((d_R(u) + d_R(v))x^{d_R(e)}\right)$$

$$= (|E_1(R)| + |E_2(R)| + |E_3(R)| + |E_4(R)| + |E_5(R)| + |E_6(R)| + |E_7(R)| + |E_8(R)|)\left((d_R(u) + d_R(v))x^{d_R(e)}\right)$$

$$= 2(3x) + 5(4x^2) + 2(5x^3) + 9(4x^2) + 14(5x^3) + 4(6x^4) + 4(6x^4) + 2(7x^5)$$

$$= 14x^5 + 60x^4 + 80x^3 + 56x^2 + 6x.$$

$KCD_2(R)$ being first derivative of $KCD_2(R,x)$ at $x=1$, gives

$$KCD_2(R) = \frac{\partial}{\partial x}(KCD_2(R,x))|_{x=1}$$

$$= \frac{\partial}{\partial x}(14x^5 + 60x^4 + 80x^3 + 56x^2 + 6x)|_{x=1}$$

$$= 668.$$

5.3 KCD Polynomials of Amphotericin B

Graph A in figure 3 represents the molecular graph of amphotericin B. It has $|V(A)| = 65$ and $|E(A)| = 67$. For $i, j \geq 1$, $uv \in E(A)$ and $(d_A(u), d_A(v)) = (i,j)$ and let $E(A) = \cup_{i=1}^{6} E_i(A)$.

Figure.3 Molecular graph of amphotericin B

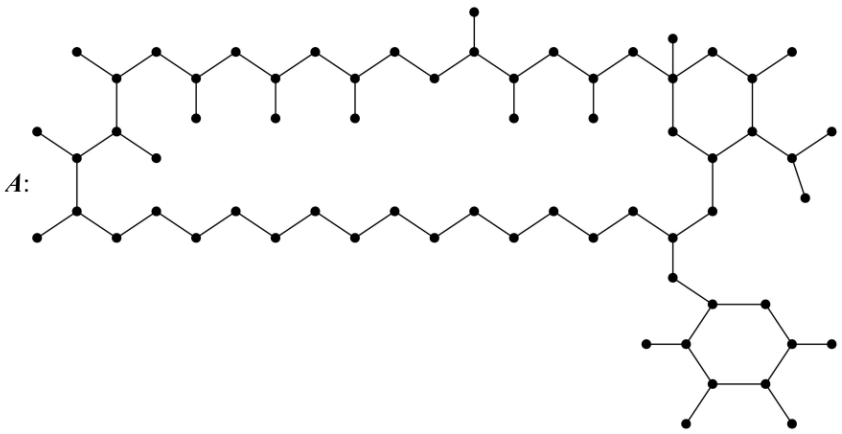

Table.3 Edge partition of $E(A)$.

$E_i = E_i(A)$	$d_A(u) = i$	$d_A(v) = j$	$d_A(e)$	$\lvert E_i(A)\rvert$
E_1	1	3	2	17
E_2	1	4	3	1
E_3	2	2	2	14
E_4	2	3	3	21
E_5	2	4	4	3
E_6	3	3	4	11

Theorem 5.3 *For the molecular graph of amphotericin B,*

$$a.) \quad KCD_1(A,x) = 14x^6 + 22x^5 + 45x^4 + 22x^3 + 31x^2 \quad and \quad KCD_1(A) = 502.$$

$$b.) \quad KCD_2(A,x) = 84x^4 + 110x^3 + 124x^2 \quad and \quad KCD_2(A) = 914.$$

Proof. With the help of Eq. (5.1) and table 3, we obtain

$$KCD_1(A,x) = \sum_{e=uv\in E(A)} (x^{d_A(u)+d_A(v)} + x^{d_A(e)})$$

$$= (\sum_{e=uv\in E_1(A)} + \sum_{e=uv\in E_2(A)} + \sum_{e=uv\in E_3(A)} + \sum_{e=uv\in E_4(A)} +$$

$\sum_{e=uv\in E_5(A)}$

$$+\sum_{e=uv\in E_6(A)}\left(x^{d_A(u)+d_A(v)}+x^{d_A(e)}\right)$$

$$=(|E_1(A)|+|E_2(A)|+|E_3(A)|+|E_4(A)|+|E_5(A)|$$
$$+|E_6(A)|)\left(x^{d_A(u)+d_A(v)}+x^{d_A(e)}\right)$$

$$=17(x^4+x^2)+(x^5+x^3)+14(x^4+x^2)+21(x^5+x^3)+3(x^6+x^4)$$
$$+11(x^6+x^4)$$
$$=14x^6+22x^5+45x^4+22x^3+31x^2.$$

$KCD_1(A)$ being first derivative of $KCD_1(A,x)$ at $x=1$, gives

$$KCD_1(A)=\frac{\partial}{\partial x}(KCD_1(A,x))|_{x=1}$$
$$=\frac{\partial}{\partial x}(14x^6+22x^5+45x^4+22x^3+31x^2)|_{x=1}$$
$$=502.$$

Using Eq. (5.2) and table 3, we get

$$KCD_2(A,x)=\sum_{e=uv\in E(A)}(d_A(u)+d_A(v))x^{d_A(e)}$$
$$=(\sum_{e=uv\in E_1(A)}+\sum_{e=uv\in E_2(A)}+\sum_{e=uv\in E_3(A)}+\sum_{e=uv\in E_4(A)}+$$
$$\sum_{e=uv\in E_5(A)}+\sum_{e=uv\in E_6(A)})\left((d_A(u)+d_A(v))x^{d_A(e)}\right)$$
$$=(|E_1(A)|+|E_2(A)|+|E_3(A)|+|E_4(A)|+|E_5(A)|$$
$$+|E_6(A))\left((d_A(u)+d_A(v))x^{d_A(e)}\right)$$
$$=17(4x^2)+(5x^3)+14(4x^2)+21(5x^3)+3(6x^4)+11(6x^4)$$
$$=84x^4+110x^3+124x^2.$$

$KCD_2(A)$ being first derivative of $KCD_2(A,x)$ at $x=1$, gives

$$KCD_2(A)=\frac{\partial}{\partial x}(KCD_2(A,x))|_{x=1}$$
$$=\frac{\partial}{\partial x}(84x^4+110x^3+124x^2)|_{x=1}$$
$$=914.$$

6. QSPR/QSAR Analysis of Drugs Used for COVID-19 and Mucormycosis

This segment concentrates to learn the QSPR/QSAR efficacy of COVID-19 antiviral drugs. Five degree based topological indices given by Eqs. (3.1), (3.2), (3.3), (3.4) and (3.5) and four physicochemical properties: molecular weight (MW), topological polar surface area (TPSA), heavy atom count (HAC) and complexity (C) of COVID-19 antiviral drugs are used for estimation.

AIIMS/ICMR-COVID-19 National Task Force jointly with Ministry of Health & Family Welfare, Government of India on $22nd$ April 2021 and Government of Karnataka on $01st$ May 2021 had brought forward new clincial guidelines regarding medication in adults having COVID-19. These guidelines categorises COVID-19 patients in mild, moderate and severe disease groups and the treatment is suggested accordingly. In addition, IMA has proposed guidelines for diagnosing and managing mucormycosis infected COVID-19 patients. Thus, we conduct the present QSPR/QSAR analysis in three different subsections viz. mild disease category, moderate/severe disease category (since the antiviral drugs used for moderate and severe disease are same with variation in dosages, we consider these two categories together) and black fungus disease category.

6.1 Mild Disease Category for COVID-19

This subsection studies the QSPR/QSAR inspection of COVID-19 drugs used in mild disease category. The patients in the mild disease category are home isolated. Based on the symptoms experienced by patients antiviral drugs administered are ivermectin, hydroxychloroquine, budesonide, cetirizine, codeine (anti-tussive cough syrup) and dextromethorphan (**Katzung, 2018**).

The table 4 contains the details of physicochemical properties related to antiviral drugs used for COVID-19 in mild disease category, table 5 lists the computed values of topological indices for them. Table 6 gives the details of correlation coefficient (r) values for topological indices and physicochemical properties of antiviral drugs used for COVID-19 treatment in mild disease cateogry with its plot represented in figure 4.

Table.4 Details of antiviral drugs for mild disease cateogry.

Drugs	MW	TPSA	HAC	C
Ivermectin	875.1	170	62	1680
Hydroxycholoroquine	335.9	48.4	23	331
Budesonide	430.5	93.1	31	862
Cetirizine	461.8	53	29	443
Codeine	299.4	41.9	22	509
Dextromethorphan	271.4	12.5	20	370

Table.5 Details of topological indices for mild disease cateogry.

Drugs	$R(G)$	$R_k(G)$	$GA(G)$	$KCD_1(G)$	$KCD_2(G)$
Ivermectin	28.92	162.4712	64.5366	538	1066
Hydroxycholoroquine	11.1345	53.6864	23.375	172	292
Budesonide	18.3294	88.6737	32.0776	288	646
Cetirizine	13.131	65.59	14.1777	232	364
Codeine	10.6638	66.5939	25.3846	220	466
Dextromethorphan	9.7431	56.7767	22.4918	186	376

Figure.4 Plot of r values for mild disease cateogry.

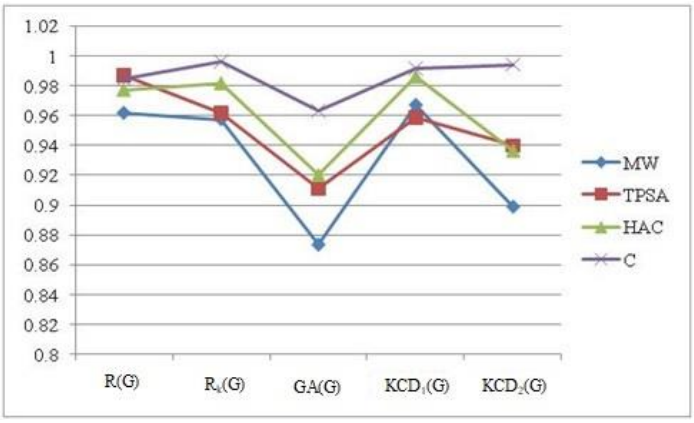

Table.6 Details of r values for topological indices and COVID-19 drugs for mild disease cateogry.

Properties: Mild disease	$\boldsymbol{R(G)}$	$\boldsymbol{R_k(G)}$	$\boldsymbol{GA(G)}$	$\boldsymbol{KCD_1(G)}$	$\boldsymbol{KCD_2(G)}$
MW	0.962172	0.957847	0.873676	**0.96748**	0.89921
TPSA	**0.987174**	0.961796	0.911132	0.95896	0.94009
HAC	0.977741	0.982051	0.920615	**0.98662**	0.93705
C	0.984356	**0.996299**	0.963069	0.99165	0.99414

The observation of table 6 and figure 4 indicates that the appropriate fitting model for MW, TPSA, HAC and C are

1. First KCD index for MW with $r = 0.96748$.
2. Randić index for TPSA with $r = 0.987174$.
3. First KCD index for HAC with $r = 0.98662$.
4. General Randić index for C with $r = 0.996299$.

6.2 Moderate/Severe Disease Category for COVID-19

Present subsection studies the QSPR/QSAR investigation of COVID-19 drugs in moderate/severe disease category. The patients categorised by moderate disease are admitted in ward and for severe disease in ICU (Intensive care unit). Monitoring the condition of patients the therapeutics used in precribed dosage are methylprednisolone, dexamethasone, heparin as required. Further, based on specific circumstances EUA (Emergency Use Authorization) of remdesivir is considered only in patients having moderate to severe disease.

The table 7 contains the details of physicochemical properties related to antiviral drugs used for COVID-19 in moderate/severe disease category, table 8 registers the calculated values of topological indices for them, table 9 features corresponding r values and figure 5 shows the r values plotted.

Table.7 Details of antiviral drugs for moderate/severe disease cateogry.

Drugs	MW	TPSA	HAC	C
Methylprednisolone	374.5	94.8	27	754
Dexamethasone	392.5	94.8	28	805
Heparin	1134.9	652	70	2410
Remdesivir	602.6	204	42	1010

Table.8 Details of topological indices for moderate/severe disease cateogry.

Drugs	$R(G)$	$R_k(G)$	$GA(G)$	$KCD_1(G)$	$KCD_2(G)$
Methylprednisolone	12.9631	79.8292	29.9388	274	624
Dexamethasone	12.5811	76.28	35.9746	260	572
Heparin	30.7894	170.9518	66.2818	586	1178
Remdesivir	19.508	104.0234	42.2832	344	668

Table.9 Details of r values for topological indices and COVID-19 drugs for moderate/severe disease cateogry.

Properties: Moderate/severe disease	$R(G)$	$R_k(G)$	$GA(G)$	$KCD_1(G)$	$KCD_2(G)$
MW	0.995439	**0.998475**	0.990877	0.996886	0.979687
TPSA	0.982285	0.995616	0.984135	**0.998161**	0.994177
HAC	**0.998651**	0.996445	0.988822	0.992748	0.969111
C	0.969431	0.987904	0.981464	0.99257	**0.99457**

Figure.5 Plot of r values for moderate/severe disease cateogry.

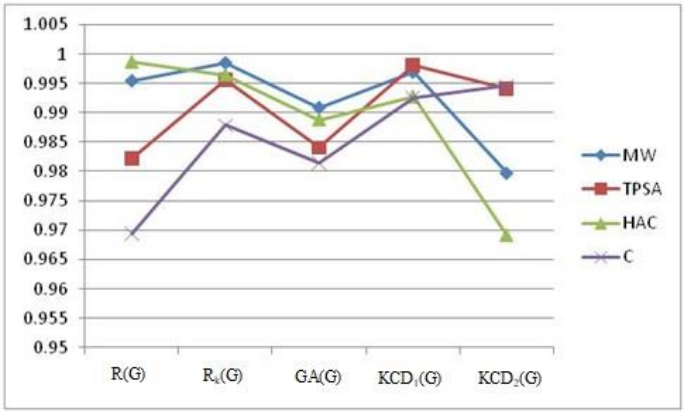

The inspection of table 9 and figure 5 reveals that the best fitting model for MW, TPSA, HAC and C are

1. General Randić index for MW with $r = 0.998475$.
2. First KCD index for TPSA with $r = 0.998161$.

3. Randić index for HAC with $r = 0.998651$.

4. Second KCD index for C with $r = 0.99457$.

6.3 Mucormycosis (Black Fungus) Disease Category

The current subsection deals with QSPR/QSAR examination of drugs used to treat mucormycosis (black fungus) disease category. This rare disease caused by moulds of mucormycetes these days is observed in recovered, recovering and acute COVID-19 patients. Admist second wave of COVID-19, the increased frequency of fungal patients has become a cause of worry (**Sahoo *et al.*, 2021**). The therapeutics suggested by IMA for black fungus disease and considered for present QSPR/QSAR analysis are isavuconazole, posaconazole and amphotericin B.

Details related to physicochemical properties of the medicines used in treatment of black fungus are mentioned in table 10, where as table 11 contains the estimated topological indices values for them. The correlated r values obtained for these drugs and their considered properties are placed in table 12 and plotted in figure 6.

Table.10 Details of drugs used for black fungus.

Drugs	MW	TPSA	HAC	C
Isavuconazole	437.5	116	31	657
Posaconazole	700.8	112	51	1170
Amphotericin B	924.1	320	65	1670

Table.11 Details for topological indices of drugs used for black fungus.

Drugs	$R(G)$	$R_k(G)$	$GA(G)$	$KCD_1(G)$	$KCD_2(G)$
Isavuconazole	14.9018	80.5588	33.6296	264	504
Posaconazole	24.724	135.7105	55.5654	442	836
Amphotericin B	30.6153	152.3694	63.9264	502	914

Table.12 Details of r values for topological indices and drugs for black fungus.

Properties: Black fungus disease	$R(G)$	$R_k(G)$	$GA(G)$	$KCD_1(G)$	$KCD_2(G)$
MW	**0.995394**	0.96824	0.978915	0.973353	0.95649
TPSA	**0.775145**	0.667058	0.701318	0.6828	0.634133
HAC	**0.999122**	0.980345	0.98853	0.984331	0.97087
C	**0.990762**	0.957462	0.96996	0.963401	0.944052

Figure.6 Plot of r values for black fungus disease category.

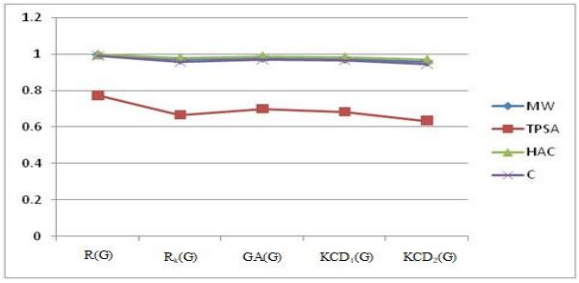

The r values in table 12 and plot of figure 6 reveals that all the topological indices considered are closely correlated with the r values ranging from 0.944052 to 0.999122 for MW, HAC and C. In case of TPSA the dip is observed for r values from 0.634133 to 0.775175. Overall analysis of table 12 indicates Randić index to be a good fit, followed by geometric-arithmetic index and first KCD index with good predicting capacity.

6.4 Results and Discussion

Table.13 Details of average of r values .

Average r	$R(G)$	$R_k(G)$	$GA(G)$	$KCD_1(G)$	$KCD_2(G)$
Mild	**0.977861**	0.974498	0.917123	0.976178	0.942623
Moderate/ Severe	0.986452	0.99461	0.986325	**0.995091**	0.984356
Black fungus	**0.94011**	0.893276	0.909681	0.900971	0.87639

Figure.7 Plot of average r values.

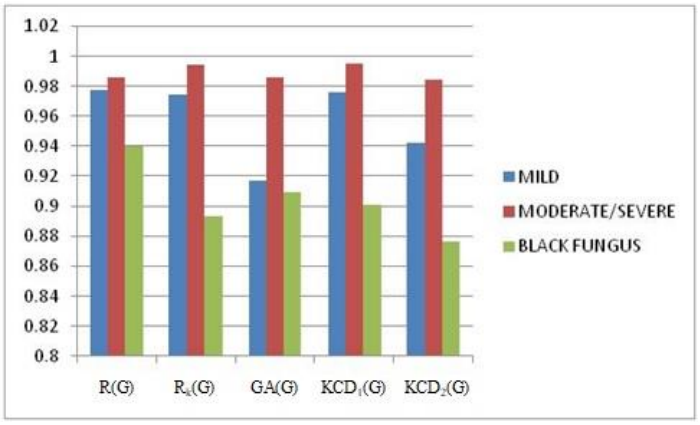

The present QSPR/QSAR study focuses on drugs used for the medication of COVID-19 and mucormycosis patients using degree based topological indices. The topological indices $R(G)$, $R_k(G)$, $GA(G)$, $KCD_1(G)$ and $KCD_2(G)$ used for this purpose have shown good performance in all the three categories: mild disease, moderate/severe disease and black fungus disease.

The observations from 1 to 8 indicates that every topological index used has a particular predicting power so that exactly use of only one topological index to determine the QSPR/QSAR analysis of one specific category

for mild or moderate/severe disease category is difficult. This emphasises the use of each topological index. For instance, in mild disease category MW and HAC are better predicted by first KCD index where as Randić index shows good performance with TPSA and general Randić index for C. In the similar way, for moderate/severe disease category MW is better predicted by general Randić index, TPSA by first KCD index, HAC by Randić index and C by second KCD index. Black fungus disease category is better predicted by Randić index with close competitors being geometric-arithmetic index

and first KCD index. One shortcoming throughtout the analysis is the dip in the predicting power of all the considered topological indices observed for TPSA in black fungus disease category with the considerable r value.

Finally, the table 13 and figure 7 gives the clear picture of the analysis conducted for drugs used to treat COVID-19 and black fungus disease. Overall observation concludes Randić index to better performer for mild disease category with average $r = 0.977861$, first KCD index is the best performer for moderate/severe disease category with average $r = 0.995091$ (maximum average r value) and for black fungus Randić index is the good performer with average $r = 0.94011$.

7. Conclusion

To analyse the therapeutic effect of a newly designed drug mainly its properties are essential which can be correlated with representative molecular descriptor to conduct the necessary QSPR/QSAR analysis. These molecular descriptors are computed using various techniques. Presently, we use edge partition technique to obtain the topological index of ivermectin, remdesivir and amphotericin B using newly defined KCD polynomials.

Proceeding with the QSPR/QSAR analysis of the antiviral drugs used to treat COVID-19 and therapeutics used for black fungus disease. The analysis was separately carried out for drugs used to treat COVID-19 patients considering mild disease category and moderate/severe disease category, followed by medications used for fungal infected patients of black fungus disease. The final conclusion is that, all the topological indices considered for present study are prominent in their own way for QSPR/QSAR analysis of drugs used in medication of COVID-19 as well as black fungus disease. Among the surveyed topological indices Randić index and first KCD index are the centre of attention with average correlation values $r = 0.977861$ for mild disease category, $r = 0.94011$ for black fungus disease and $r = 0.995091$ (highest average r value) for moderate/severe disease category respectively. The examined data in the current study will be able to help in the efficiency detection of drugs for medication of COVID-19 and black fungus disease.

8. Acknowledgement

The authors are grateful to Karnatak University, Dharwad, Karnataka, India for the support through University Research Studentship (URS), No.KU/Sch/URS/2020-21/1103 dated: 21/12/2020.

References

1. Balban, A.T., (1976). Chemical Applications of Graph Theory. Academic Press.
2. Bollobás, B & Erdös, P., (1998). Graphs of extremal weights. Ars Combinatoria, 50, 225-233.
3. Fath-Tabar, G., (2009). Zagreb polynomial and PI indices of some nano structures. Digest Journal of Nanomaterials and Biostructures, 4, 189-191.
4. Ghosh, A., Nundy, S. & Mallick T. K., (2020). How India is dealing withCOVID-19 pandemic. Sensors International, 1, 100021.
5. Gutman, I., Klavžar, S., Petkovsek, M. & Zigert P., (2001). On Hosoya polynomials of benzenoid graphs. MATCH Communications in Mathematical and in Computer Chemistry, 43, 49-66.
6. Gutman, I., Ruščič, B., Trinajstić, N. & Wilcox, F. C., (1975). Graph theory and molecular orbitals. XII. Acyclic polyenes. Journal of Chemical Physics, 62, 3399–3405.

7. Gutman, I & Trinajstić, N., (1972). Graph theory and molecular orbitals. Total π-electron energy of alternant hydrocarbons. Chemical Physics Letters, 17, 535–538.
8. Harary, F., (1969). Graph Theory. Addison – Wesely, Reading, Mass.
9. Hosamani, S.M., (2020). Quantitative structure property analysis of anti-covid-19drugs, arXiv:2008.07350.
10. Hosoya, H., (1971), Topological index. A newly proposed quantitycharacterizing the topological nature of structural isomers of saturated hydrocarbons. Bulletin of the Chemical Society of Japan, 44(9), 2332–2339.
11. Katzung, B.G., (2018). Basic & Clinical Pharmacology. McGraw-Hill, NewYork, 14th ed., Chap. 31,pp. 570.
12. Kirmani, S.A.K., Ali, P. & Azam, F., (2020). Topological indices and QSPR/QSAR analysis of some antiviral drugs being investigated for the treatment of COVID-19 patients. International Journal of Quantum Chemistry, 121(9), e26594.
13. Lu, H., Stratton, C.W & Tang, Y., (2020). Outbreak of pneumonia of unknown etiology in Wuhan, China: The mystery and the miracle. Journal of Meddical Virology, 401–402.
14. Mirajkar, K. G & Morajkar, A., (2020). KCD indices and coindices of graphs.Ratio Mathematica, 39, 165–186.
15. Randić, M., (1975). On characterization of molecular branching. Journal of American Chemical Society, 97, 6609–6615.
16. Ranjan, R., Sharma, A. & Verma, M.K., (2021). Characterization of the second wave of COVID-19 in India. *medRxiv*.
17. Samui, P., Mondal, J. & Khajanchi, S., (2020), A mathematical model for COVID-19 transmission dynamics with a case study of India. Chaos Solitons Fractals, 140, 110173.
18. Sahoo, J. P., Panda, B., Mishra, A.P. & Samal, K. C., (2021). The unseen fungal infections - An extra thrust aggravating COVID second wave in India. Biotica Research Today, 3(5), 354–356.
19. Stevanović, D., (2001). Hosoya polynomial of composite graphs. Discrete Mathematics, 235(1-3), 237–244.
20. Vukičević, D. & Furtula, B., (2009). Topological index based on the ratios ofgeometrical and arithmetical means of end-vertex degrees of edges. Journal of Mathematical Chemistry, 46, 1369–1376.
21. Wiener, H., (1947). Structural determination of paraffin boiling points, Journal of American Chemical Society, 69(1), 17–20.